Title page

Title

Prediction model for extensive ductal carcinoma in situ around early stage invasive breast cancer

Authors

Floortje M. Knuttel, MD[1], Bas H.M. van der Velden, MSc[2], Claudette E. Loo, MD[3], Sjoerd G. Elias, MD PhD[4], Jelle Wesseling, MD PhD[5], Maurice A.A.J. van den Bosch, MD PhD[1], Kenneth G.A. Gilhuijs, PhD[2]

Affiliations

[1] Department of Radiology, University Medical Center Utrecht, Utrecht, The Netherlands

[2] Image Sciences Institute, University Medical Center Utrecht, Utrecht, The Netherlands

[3] Department of Radiology, Netherlands Cancer Institute, Amsterdam, the Netherlands

[4] Julius Center for Health Sciences and Primary Care, University Medical Center Utrecht, Utrecht, The Netherlands

[5] Department of Pathology, Netherlands Cancer Institute, Amsterdam, The Netherlands

Structured abstract

Objectives Ductal carcinoma in situ (DCIS) is a risk factor for incomplete resection of breast cancer. Especially extensive DCIS (E-DCIS) or extensive intraductal component often results in positive resection margins. Detecting DCIS around breast cancer prior to treatment may therefore alter surgery. The purpose of this study was to develop a prediction model for E-DCIS around early-stage invasive breast cancer, using clinicohistopathological and dynamic contrast-enhanced magnetic resonance imaging (DCE-MRI) features.

Materials and Methods DCE-MRI and local excision were performed in 322 patients with 326 ductal carcinomas. Tumors were segmented from DCE-MRI, followed by 3D extension of the margins with 10 mm. Tissue density and enhancement features in these extended margins were automatically extracted from the MR-images. Clinicohistopathological features were also obtained. Principal component analysis and multivariable logistic regression were used to develop a prediction model for E-DCIS. Discrimination and calibration were assessed and bootstrapping was applied for internal validation.

Results E-DCIS occurred in 48/326 tumors (14.7%). Incomplete resection occurred in 56.3% of these E-DCIS-positive versus 9.0% of E-DCIS-negative tumors ($p<0.001$). Five components with eigenvalue exceeding 1 were identified; two were significantly associated with E-DCIS. The first, positively associated, component expressed early and overall enhancement in the 10 mm tissue margin surrounding the MRI-visible tumor. The second, positively associated, expressed human epidermal growth factor receptor 2 (HER2) and tissue density around the MRI-visible tumor.. The AUC-value was 0.79 (0.76 after bootstrapping).

Conclusions HER2 status, early and overall enhancement in the 10 mm margin around the MR-visible tumor and density in the 10 mm around the MR-visible tumor were associated with E-DCIS.

Keywords

Breast cancer

Magnetic resonance imaging

MRI

Ductal carcinoma in situ

DCIS

Breast-conserving surgery

Resection margins

Prediction model

Introduction

Breast cancer is increasingly diagnosed at an early stage, which is the result of improved imaging techniques and screening programs(1-3). Due to the increasing incidence of early-stage breast cancer, breast-conserving therapy is the most preferred treatment. The presence of ductal carcinoma in situ (DCIS) increases the risk of positive resection margins(4-6). Positive margins for either invasive carcinoma or DCIS are associated with an increased risk of local or distant recurrence(7-10). Re-excision is often required in case of positive resection margins, deforming the breast, increasing the risk of complications and leading to patients' anxiety(11).

Kinetic analysis of dynamic contrast-enhanced MRI (DCE-MRI) features enables discrimination of benign and malignant lesions(12). The sensitivity of DCE-MRI for detecting DCIS is higher than the sensitivity of conventional imaging modalities, and DCE-MRI is superior in assessing the extent of DCIS(13, 14). However, the specificity of MRI for detecting DCIS and invasive cancer is low to moderate(15, 16). Performing DCE-MRI prior to surgery in patients diagnosed with DCIS has not been proven to beneficially influence outcome so far. Apparently, patients with DCIS are still at risk of incomplete surgery due to undetected disease. Conversely, MRI may result in increased mastectomy rates due to uncertainty about the relevance of unexpected findings(17). Despite the ability of DCE-MRI to detect DCIS, different imaging protocols or combining MRI findings with other tumor characteristics seem necessary to improve preoperative detection of DCIS components.

Knowing the risk of positive resection margins due to the presence of DCIS around the primary tumor may guide surgical treatment in the future.. For example, during surgical resection, the margin width can be increased to prevent re-excision. Especially patients with extensive DCIS around the tumor are important to identify because their tumors are frequently associated with malignant tissue beyond the intended surgical margin of 10 mm from the tumor border(18, 19). Using DCE-MRI to predict the presence of DCIS in the tissue surrounding the tumor has, to our knowledge, not been done so far. We hypothesize that computer-extracted features derived from DCE-MRI may improve the

detection of DCIS surrounding invasive breast cancers. The purpose of this study is to use patient and tumor characteristics and computer-extracted DCE-MRI features for optimal prediction of the presence of extensive DCIS surrounding early-stage invasive breast cancer.

Materials and methods

Patients

A subset of 322 patients with 326 pathologically proven invasive ductal carcinomas was selected from the prospective Multimodality Analysis and Radiological Guidance IN breast-conServing therapy (MARGINS) study. Patients were consecutively included between 2000 and 2008. The ethics committee of the Netherlands Cancer Institute (Amsterdam, the Netherlands) approved the MARGINS study and all participants signed informed consent. The aim of the MARGINS study was to assess whether adding preoperative MRI to conventional imaging improves the accuracy of staging and localization of breast cancer. Included patients were diagnosed with invasive breast cancer for which breast-conserving surgery was indicated based on physical examination, mammography and ultrasound (US). The largest tumor diameter on US was recorded. Breast cancer was confirmed by fine needle aspiration cytology and/or core needle biopsy. All patients underwent additional preoperative contrast-enhanced MR imaging(20, 21). Patients who received neoadjuvant chemotherapy were excluded as this may change tumor characteristics. Patients who underwent mastectomy due to additional findings on MRI were excluded, because this implies wider margins than local excision. Age was obtained from the moment of breast cancer diagnosis.

MRI acquisition

Patients underwent MR imaging with a 1.5 T scanner (Magnetom, Siemens Medical Systems, Erlangen, Germany). Patients were positioned in prone position and images were acquired using a double-breast array coil (CP Breast Array, four channels; Siemens). Both non-contrast and contrast-enhanced MRI scans were performed. Contrast-enhanced scans were generated after intravenous injection with the gadolinium-based contrast agent gadoteridol (Prohance, Bracco-Byk Gulden, Konstanz, Germany) at 0.1 mmol/kg body weight. Five consecutive scans with intervals of 9 0 s were performed, one before and four after contrast administration. The imaging parameters were 3D coronal T1-weighted

sequence, repetition time 8.1 ms, echo time 4.0 ms, isotropic voxels of 1.35 x 1.35 x 1.35 mm^3, without fat suppression.

Extraction of MRI features

Tumors were automatically segmented from MR images and a dedicated breast radiologist established the largest tumor diameter after measuring diameter in three orthogonal directions. Volumetric tumor segmentation was performed automatically as previously reported by Alderliesten et al.(22). Tumor margins were automatically extended with 10 mm in 3D. First, the breast region was segmented to prevent inclusion of pectoral muscle, skin and air outside the breast in the extended margins(23). Parenchymal density in the extended margins was calculated as the ratio of the volume of fibroglandular tissue over total volume in the extended margin. The fibroglandular tissue was automatically segmented using previously reported methodology by Klifa et al.(24). Early, late and overall enhancement in these extended margins were derived from subtraction images, which were calculated per fibroglandular tissue voxel and averaged (*figure 1 and 2*)(25). Early enhancement was defined as the percentage signal increase between pre-contrast and first post-contrast scan, $100\%*(S_1-S_0)/S_0$, late enhancement between the late post-contrast and first post-contrast scan, $100\%*(S_2-S_1)/S_1$, and overall enhancement between the pre-contrast and the late post-contrast scan $100*(S_2-S_0)/S_0$. S_0 denotes the image intensity in the pre-contrast image, S_1 in the first post-contrast image and S_2 in the last post-contrast scan. Signal Enhancement Ratio (SER) was defined as the ratio between early and overall enhancement, $100\%*(S_1-S_0)/(S_2-S_0)$(26). The median SER values of the fibroglandular tissue voxels were used in the analysis to prevent impact of noise.

Breast cancer treatment and histopathologic analysis

Patients underwent wide-local excision, with intended tumor-free margins of at least 1 cm. The applied surgical technique was adopted from Aspegren, who described wide local excisions extending from skin to basal fascia(27). Margin status (positive vs. negative), estrogen receptor (ER) status,

progesterone receptor (PR) status, human epidermal growth factor receptor 2 (HER2) status, Nottingham histologic grade(28) and presence and amount of DCIS around the invasive tumor were assessed. Positive margins were defined as tumor present in the edge of the excision specimen, either focally (less than two low power fields) or extensively (in two or more low power fields). More than 10% staining of tumor cells resulted in positive ER and PR status. HER2 receptor was considered positive when immunohistochemistry was scored at least 3 and in situ hybridization showed gene amplification. The extent of DCIS in the surrounding breast tissue was estimated as none, minimal, moderate or extensive by an experienced breast pathologist. Extensive DCIS (E-DCIS) was defined as prominent DCIS within the confines of the invasive tumor (typically occupying at least 25% of the tumor) and DCIS in the grossly normal adjacent breast tissue, or lesions composed primarily of DCIS with one or more foci of invasive carcinoma(19). The amount of DCIS was considered minimal if DCIS was present in up to 5 ducts and moderate if the amount was beyond the amount of minimal DCIS but not sufficient to meet the criteria for E-DCIS. E-DCIS was the primary endpoint of this study. The presence of E-DCIS was scored dichotomously; yes (extensive DCIS versus no (none, minimal or moderate DCIS).

Statistical analysis

For continuous variables mean and standard deviations (SD) or median and interquartile range were calculated. Categorical variables were displayed as numbers with percentages. Associations between variables and the presence of E-DCIS in the tumor margin were assessed with independent-t tests (continuous normally distributed variables), Mann-Whitney U-tests (continuous non-normally distributed variables) or Fisher's exact tests (categorical variables). Normality was tested with Q-Q plots and Kolmogorov-Smirnov tests. Single imputation was performed for missing data, using the expectation-maximization method(29). Less than 5% of data was missing, so this method was suitable for our dataset.

Principal component analysis (PCA) with varimax rotation was performed to determine factor loadings and to cluster variables in components. PCA results in completely independent components(30). PCA instead of multivariable analysis of the original variables was used to prevent overfitting of the prediction model. Only variables known prior to surgical treatment were included in the PCA to reflect the typical pre-treatment workflow. The MRI-variables included in the PCA were: tumor size measured on MRI and density, early, late and overall enhancement and SER in the 10 mm margin surrounding the tumor. Included patient characteristics and variables derived from conventional imaging were: age, ER status, PR status, HER2 status, suspicious calcifications and difference between largest tumor diameter on MRI and on US. Components with eigenvalue larger than 1.0 were selected and labeled, variables with relatively high factor loadings were identified. The Kaiser-Meyer-Olkin Measure of Sampling Adequacy (KMO) was performed to assess the amount of common variance in the dataset. A value of > 0.5 is considered sufficient for PCA. Bartlett's test was performed as well, in order to assess whether data were independent or not(31).

Individual factor scores for the selected components were calculated and stored. These factor scores were used as covariates to assess the association with E-DCIS using multivariable logistic regression in order to develop a prediction model(32). A receiver operating characteristic (ROC) curve was generated. The area under the curve (AUC) was calculated to assess the discriminative ability of the prediction model. Calibration was assessed with the Hosmer-Lemeshow test and a calibration plot. Bootstrapping with 1000 iterations was used for internal validation and applied to the multivariable model. The shrinkage factor was used to calculate the final AUC-value(33). No external validation was performed. A two-sided p-value of < 0.05 was assumed statistically significant in all analyses. SPSS (IBM SPSS Statistics, version 20.0, Armonk, NY) was used for PCA. Multivariable logistic regression and bootstrapping were performed with R statistics (version 3.1.1, Vienna, Austria).

Results

Patient characteristics

The mean age of included subjects was 57.9 ± 9.7 years (range 32 - 84). E-DCIS was detected in 48 tumors (14.7%) (*table 1*). In this group, positive resection margins occurred significantly more often than in the group without DCIS around the tumor, 27/48 (56.3%) versus 25/278 (9.0%) ($p < 0.001$). Univariable analysis showed that tumors surrounded by E-DCIS occurred in younger patients, were less frequently PR-positive, more frequently triple positive, larger on MRI, surrounded by denser breast tissue, showed more early enhancement, and were less frequently of low histologic grade.

Principal component analysis

The PCA resulted in five components with eigenvalues larger than 1 (*table 2*). The cumulative explained variance of these factors was 73.03%. The calculated KMO was 0.468 and Barlett's test was significant ($p < 0.001$). Component 1 was represented by early and overall enhancement and was named *enhancement 1*. Component 2 was correlated with the other two enhancement features; late enhancement and SER and was called *enhancement 2*. Component 3 was correlated with largest tumor diameter established on MRI and the difference between largest diameter on MRI and US (*Tumor size*). ER and PR status were represented in component 4 (*ER/PR status*). Density combined with HER2 status was represented in component 5 (*Density/HER2*).

Prediction model

According to the multivariable logistic regression model, *Enhancement 1* (OR 1.51 (95%-CI 1.09-2.10), p=0.013) and *Density/HER2* (OR 2.38 (95%-CI 1.75-3.23) p<0.001) were positively and significantly associated with E-DCIS. Factor loadings of both early enhancement and overall enhancement were positive, indicating that the risk of E-DCIS increases with increasing early and overall enhancement. Because of positive factor loadings, patients with dense breast tissue around the MRI visible tumor

and a positive HER2 receptor are at increased risk of E-DCIS (*table 3*). The logistic regression model yielded an ROC curve with an AUC of 0.79 (95%-CI 0.72 - 0.85) (*figure 3*). The Hosmer-Lemeshow test was not significant (p = 0.907), indicating a good fit of the model, which was graphically supported by the calibration plot (*figure 4*). Bootstrapping resulted in a final AUC-value of 0.76 (shrinkage factor 0.89).

Discussion

The multivariable regression model obtained after PCA showed that patients with more early enhancement and more overall enhancement in a margin of 10 mm around the MR-visible tumor, higher tissue density in a 10 mm margin around the MRI visible tumor and positive HER2 receptor are at increased risk of E-DCIS around the tumor. The prediction model had a bootstrapped AUC-value of 0.76. Patients with E-DCIS around their invasive tumor had significantly more often positive resection margins (56.3% vs. 9.0%, $p < 0.001$).

Being able to anticipate E-DCIS may improve the rate of incomplete resections. The reported model is a first initiative to predict the occurrence of E-DCIS around invasive breast cancer by combining MRI features with clinical and histopathological features. If the presence of E-DCIS is likely, appropriate steps may be taken. In case of Breast Carcinoma of Limited Extent (non-BCLE, i.e. tumors with malignant tissue at or beyond 10 mm from the edge of the tumor(18)) excision of the primary tumor with a 10 mm margin followed by radiotherapy may be sufficient. In case of non-BCLE, excision could be performed with wider margins. Thus, knowing the risk of E-DCIS prior to treatment may be used to guide surgical treatment in the future. However, combining a preoperative prediction model with margin assessment during surgery would be the most optimal strategy. If only preoperative information is used, removing too much tissue is a potential risk that should be prevented. For example frozen section analysis of the resection bed(34) intra-operative touch preparation cytology(35) or optical coherence tomography(36) are techniques to assess the presence of residual disease during surgery. Conversely, the use of intraoperative margin assessment only without the ability to warn surgeons beforehand about presence of subclinical disease may result in multiple resections that are more difficult to interpret by pathologists.

Enhancement measured at two different time points after contrast injection was associated with E-DCIS. Our findings are congruent with previous research, which indicated that E-DCIS is detectable by contrast-enhanced MRI(14, 37, 38). In addition, increased parenchymal SER was related

to local recurrence in patients with DCIS by Kim et al., suggesting that parenchymal enhancement indeed implies worse surgical outcome(39). We related enhancement around the MR-visible tumor combined with patient- and tumor characteristics to the presence of E-DICS. This novel, combined approach resulted in an improved ability to pre-operatively detect E-DICS.

E-DCIS or extensive intraductal component (EIC) has been related to HER2 status in previous research as well. Somerville et al. demonstrated that the prevalence of HER2 positivity is significantly higher in IDC with an EIC than without an EIC(40). HER2 expression is more common in DCIS lesions, which also corroborates our findings(41, 42). Harada et al. assessed whether receptor status in patients diagnosed with DCIS was associated with presence of invasive disease. Their conclusion was that invasive carcinoma occurred more frequently in patients with HER2-positive DCIS, confirming our results that HER2 was found more frequently in patients with E-DCIS surrounding invasive carcinomas(43). Furthermore, HER2 positivity (in absence of anti-HER2 therapy) and E-DCIS are both associated with worse clinical outcome(19, 44), possibly explaining their relationship in our database.

Patients with E-DCIS were found to have increased tissue density around the MRI visible tumor. DCIS originates from epithelial cells from ducts in the breast. The malignant cells accumulate within the ducts and lobules. Hence, DCIS may resemble fibroglandular tissue on MRI. This is confirmed on conventional imaging by Faverly et al., who showed that non-BLCE was positively associated with calcifications or density outside the tumor border on mammography(18). We did not find a significant association between E-DCIS and suspicious calcifications in our dataset. Furthermore, high density is a risk factor for locoregional recurrence, suggesting that fibroglandular tissue surrounding the excised tumors is more likely to contain malignant disease than adipose tissue(45).

A number of limitations of this study should be considered. First, we used receptor status as determined on excision specimens. The purpose of this study was to develop a prediction model containing variables that are known prior to surgery. In our dataset, breast cancer was typically diagnosed with fine needle aspiration cytology rather than core needle biopsy (CNB). Hence, receptor status was actually established on excision specimens. Nonetheless, breast cancer diagnosis is more

often performed using CNB, which allows reliable assessment of receptor status(46). Consequently, we used post-operative receptor status as if it were known prior to surgery. This may have resulted in slightly more accurate assessment of receptor status, because the risk of misclassification due to undersampling in heterogeneous tumors with CNB was avoided. Second, the analyzed rim of tissue of 10 mm in diameter extending from the invasive tumor may have been too small, as non-BCLE particularly consists of malignant tissue outside this area. Additional tumor foci frequently occur at larger distances from the primary tumor as well(18). The reason for assessment of 10 mm was that it corresponds to typical intended surgical margins.

The developed model has a reasonable discriminative ability and is promising for risk stratification for E-DCIS and positive excision margins. We made a first attempt to incorporate both computer-derived features and clinical and histopathological features into one model. Several improvements for clinical use are possible. The presence of (E-)DCIS outside the tumor is associated with finding an intraductal component on CNB. Hence, adding the presence of DCIS on CNB to the model may further increase the discriminative ability of the model(47). As fine needle aspiration cytology was used in many included MARGIN patients, we could not add this variable to our analyses. Additional MRI techniques such as diffusion weighted imaging (DWI) could also be tested for their ability to detect disease components. Thus far, this technique has been used to discriminate between DCIS, invasive tumor and benign lesions, such that a contrast agent may potentially even be omitted(48, 49). However, the spatial resolution of DWI is currently still limited and may be improved by, e.g., high-resolution DWI(50) or MRI scanners with higher field strength.

In conclusion, we proposed a prediction model for E-DCIS around early-stage invasive breast cancer. The model considers HER2 status, early enhancement, overall enhancement and parenchymal density in a 10 mm rim around the MRI-visible lesion. Because the model is based only on pre-treatment variables, it may be suitable for surgical planning.

Tables

Table 1 Patient characteristics and association with extensive ductal carcinoma in situ around the invasive tumor.

Characteristics	All (n=326)		E-DCIS - (n=278)		E-DCIS + (n=48)		P-value
Age (y)	57.9	*±9.7*	58.5	*±9.5*	54.8	*±10.0*	**0.015**
Right side	161	*(49.4%)*	137	*(49.3%)*	24	*(50.0%)*	1.000
Tumor size US (mm)	14.0	*(10.0-19.0)**	14.0	*(10.0- 18.3)*	16.0	*(10.6-20.8)*	0.123
Tumor size MRI (mm)	17.0	*(12.8-22.0)**	16.0	*(12.0-22.0)*	19.0	*(15.0-25.0)*	**0.029**
Difference size MRI-US	2.0	*(0.0-5.0)**	2.0	*(0.0-5.0)*	3.0	*(0.0-6.6)*	0.544
Suspicious calcifications	55	*(16.9%)*	42	*(15.1%)*	13	*(27.1%)*	0.058
ER positive	273	*(83.7%)*	237	*(85.3%)*	36	*(75.0%)*	0.090
PR positive	204	*(62.6%)*	182	*(65.5%)*	22	*(45.8%)*	**0.015**
HER2 positive	48	*(14.7%)*	26	*(9.4%)*	22	*(45.8%)*	**<0.001**
Triple negative	36	*(11.0%)*	32	*(11.5%)*	4	*(8.3%)*	0.626
Triple positive	20	*(6.1%)*	12	*(4.3%)*	8	*(16.7%)*	**0.004**
Density	31.96	*±14.98*	31.15	*±15.18*	36.65	*±12.94*	**0.019**
Early enhancement	23.31	*(15.92-32.88)**	22.55	*(15.54-31.50)*	27.13	*(19.09-41.63)*	**0.021**
Late enhancement	15.41	*±9.87*	15.27	*±9.93*	16.23	*±9.58*	0.535
Overall enhancement	40.81	*(29.27-54.81)**	40.65	*(28.40-52.77)*	42.21	*(33.93-66.73)*	0.055
SER	50.54	*±20.21*	50.28	*±20.35*	52.07	*±19.54*	0.517
Positive margin	52	*(16.0%)*	25	*(9.0%)*	27	*(56.3%)*	**<0.001**
Positive SLNB	86	*(26.4%)*	73	*(26.3%)*	13	*(27.1%)*	0.861
≥4 pos. lymph nodes	15	*(4.6%)*	13	*(4.7%)*	2	*(4.2%)*	1.000
Histologic grade 1	105	*(32.2%)*	97	*(34.9%)*	8	*(16.7%)*	**0.012**
Histologic grade 3	92	*(28.2)*	76	*(27.3%)*	16	*(33.3%)*	0.390

E-DCIS: extensive ductal carcinoma in situ, *SD:* standard deviation, *US:* ultrasound, *MRI:* magnetic resonance imaging, *ER:* estrogen receptor, *PR:* progesterone receptor, *HER2:* human epidermal growth factor receptor 2, *SER:* signal enhancement ratio, *SLNB:* sentinel lymph node biopsy

* Median and interquartile range

Table 2 Factor loadings of principal component analysis with varimax rotation.

Variables	Components				
	Enhancement 1	Enhancement 2	Tumor size	ER/PR status	Density /HER2
Early enhancemnt	**.872**	-.325	.104	-.189	-.049
Overall enhancement	**.926**	.197	.096	-.156	-.117
Late enhancement	.499	**.786**	.047	-.056	-.126
SER	.249	**-.909**	-.036	-.039	-.048
Tumor diameter MRI	.152	.092	**.849**	-.082	.167
Diff. size MRI-US	-.093	-.066	**.890**	.044	-.010
ER status	-.154	.023	**-**.020	**.855**	-.098
PR status	-.009	.011	-.013	**.853**	-.140
HER2 status	.030	-.193	.055	-.137	**.762**
Density	.279	.440	-.192	.114	**.519**
Age	-.583	-.107	.172	-.118	-.307
Susp. calcifications	-.091	.096	.168	-.170	.471
Eigenvalue	2.41	1.85	1.64	1.61	1.30
Explained variance	20.10%	15.44%	13.63%	13.39%	10.48%
Cumulative variance	20.10%	35.53%	49.16%	62.55%	73.03%

ER: estrogen receptor, *PR:* progesterone receptor, *HER2:* Human Epidermal growth factor Receptor 2, *MRI: M*agnetic resonance imaging, *US:* ultrasound, *SER:* signal enhancement ratio

Table 3 Outcome of multivariable logistic regression of five components as predictors for extensive ductal carcinoma in situ.

Component	OR	95%-CI	P-value
Enhancement 1	1.51	1.09-2.10	**0.013**
Enhancement 2	0.97	0.69-1.35	0.835
Tumor size	1.33	0.98-1.79	0.068
ER/PR status	0.82	0.61-1.12	0.209
Density/HER2	2.38	1.75-3.23	**<0.001**

CI: confidence interval, *ER:* estrogen receptor*, PR:* progesterone receptor, *HER2:* Human Epidermal growth factor Receptor 2, *OR:* odds ratio

References

1. Harper S, Lynch J, Meersman SC, et al. Trends in area-socioeconomic and race-ethnic disparities in breast cancer incidence, stage at diagnosis, screening, mortality, and survival among women ages 50 years and over (1987-2005). Cancer Epidemiol Biomarkers Prev. 2009;18(1):121-31.
2. Kuhl CK**.** The Changing World of Breast Cancer: A Radiologist's Perspective. Invest Radiol. 2015.
3. Kuhl CK, Schrading S, Strobel K, et al. Abbreviated breast magnetic resonance imaging (MRI): first postcontrast subtracted images and maximum-intensity projection-a novel approach to breast cancer screening with MRI. J Clin Oncol. 2014;32(22):2304-10.
4. Barentsz MW, Postma EL, van Dalen T, et al. Prediction of positive resection margins in patients with non-palpable breast cancer. Eur J Surg Oncol. 2015;41(1):106-12.
5. Mai KT, Yazdi HM, Ford JC, Matzinger FR**.** Predictive value of extent and grade of ductal carcinoma in situ in radiologically guided core biopsy for the status of margins in lumpectomy specimens. Eur J Surg Oncol. 2000;26(7):646-51.
6. Jung W, Kang E, Kim SM, et al. Factors Associated with Re-excision after Breast-Conserving Surgery for Early-Stage Breast Cancer. J Breast Cancer. 2012;15(4):412-9.
7. Dunne C, Burke JP, Morrow M, Kell MR**.** Effect of margin status on local recurrence after breast conservation and radiation therapy for ductal carcinoma in situ. J Clin Oncol. 2009;27(10):1615-20.
8. Moran MS, Schnitt SJ, Giuliano AE, et al. Society of Surgical Oncology-American Society for Radiation Oncology consensus guideline on margins for breast-conserving surgery with whole-breast irradiation in stages I and II invasive breast cancer. J Clin Oncol. 2014;32(14):1507-15.
9. Sinn HP, Anton HW, Magener A, et al. Extensive and predominant in situ component in breast carcinoma: their influence on treatment results after breast-conserving therapy. Eur J Cancer. 1998;34(5):646-53.

10. Houssami N, Macaskill P, Marinovich ML, Morrow M**.** The association of surgical margins and local recurrence in women with early-stage invasive breast cancer treated with breast-conserving therapy: a meta-analysis. Ann Surg Oncol. 2014;21(3):717-30.

11. Wazer DE, DiPetrillo T, Schmidt-Ullrich R, et al. Factors influencing cosmetic outcome and complication risk after conservative surgery and radiotherapy for early-stage breast carcinoma. J Clin Oncol. 1992;10(3):356-63.

12. D'Orsi CJ, Sickles EA, Mendelson EB, et al. ACR BI-RADS® Atlas, Breast Imaging Reporting and Data System. Reston, VA: American College of Radiology; 2013.

13. Holland R, Hendriks JH, Vebeek AL, et al. Extent, distribution, and mammographic/histological correlations of breast ductal carcinoma in situ. Lancet. 1990;335(8688):519-22.

14. Menell JH, Morris EA, Dershaw DD, et al. Determination of the presence and extent of pure ductal carcinoma in situ by mammography and magnetic resonance imaging. Breast J. 2005;11(6):382-90.

15. Bluemke DA, Gatsonis CA, Chen MH, et al. Magnetic resonance imaging of the breast prior to biopsy. JAMA. 2004;292(22):2735-42.

16. Peters NH, Borel Rinkes IH, Zuithoff NP, et al. Meta-analysis of MR imaging in the diagnosis of breast lesions. Radiology. 2008;246(1):116-24.

17. Fancellu A, Turner RM, Dixon JM, et al. Meta-analysis of the effect of preoperative breast MRI on the surgical management of ductal carcinoma in situ. Br J Surg. 2015;102(8):883-93.

18. Faverly DR, Hendriks JH, Holland R**.** Breast carcinomas of limited extent: frequency, radiologic-pathologic characteristics, and surgical margin requirements. Cancer. 2001;91(4):647-59.

19. Schnitt SJ, Harris JR**.** Evolution of breast-conserving therapy for localized breast cancer. J Clin Oncol. 2008;26(9):1395-6.

20. Pengel KE, Loo CE, Teertstra HJ, et al. The impact of preoperative MRI on breast-conserving surgery of invasive cancer: a comparative cohort study. Breast Cancer Res Treat. 2009;116(1):161-9.

21. Pengel KE, Loo CE, Wesseling J, et al. Avoiding preoperative breast MRI when conventional imaging is sufficient to stage patients eligible for breast conserving therapy. Eur J Radiol. 2014;83(2):273-8.

22. Alderliesten T, Schlief A, Peterse J, et al. Validation of semiautomatic measurement of the extent of breast tumors using contrast-enhanced magnetic resonance imaging. Invest Radiol. 2007;42(1):42-9.

23. van der Velden BH, Dmitriev I, Loo CE, et al. Association between Parenchymal Enhancement of the Contralateral Breast in Dynamic Contrast-enhanced MR Imaging and Outcome of Patients with Unilateral Invasive Breast Cancer. Radiology. 2015:142192.

24. Klifa C, Carballido-Gamio J, Wilmes L, et al. Quantification of breast tissue index from MR data using fuzzy clustering. Conf Proc IEEE Eng Med Biol Soc. 2004;3:1667-70.

25. Gilhuijs KG, Giger ML, Bick U**.** Computerized analysis of breast lesions in three dimensions using dynamic magnetic-resonance imaging. Med Phys. 1998;25(9):1647-54.

26. Hylton NM**.** Vascularity assessment of breast lesions with gadolinium-enhanced MR imaging. Magn Reson Imaging Clin N Am. 1999;7(2):411-20, x.

27. Aspegren K, Holmberg L, Adami HO**.** Standardization of the surgical technique in breast-conserving treatment of mammary cancer. Br J Surg. 1988;75(8):807-10.

28. Elston CW, Ellis IO**.** Pathological prognostic factors in breast cancer. I. The value of histological grade in breast cancer: experience from a large study with long-term follow-up. Histopathology. 1991;19(5):403-10.

29. Enders CK**.** A Primer on Maximum Likelihood Algorithms Available for Use With Missing Data. Structural Equation Modeling: A Multidisciplinary Journal. 2001;8(1):128-41.

30. Wold S, Esbensen K, Geladi P**.** Principal component analysis. Chemometrics and Intelligent Laboratory Systems. 1987;2(1–3):37-52.

31. Dziuban CD, Shirkey EC**.** When is a correlation matrix appropriate for factor analysis? Some decision rules. Psychological Bulletin. 1974;81(6):358.

32. Moons KG, Altman DG, Reitsma JB, et al. Transparent Reporting of a multivariable prediction model for Individual Prognosis or Diagnosis (TRIPOD): explanation and elaboration. Ann Intern Med. 2015;162(1):W1-73.

33. Steyerberg EW, Harrell FE, Jr., Borsboom GJ, et al. Internal validation of predictive models: efficiency of some procedures for logistic regression analysis. J Clin Epidemiol. 2001;54(8):774-81.

34. Jorns JM, Visscher D, Sabel M, et al. Intraoperative frozen section analysis of margins in breast conserving surgery significantly decreases reoperative rates: one-year experience at an ambulatory surgical center. Am J Clin Pathol. 2012;138(5):657-69.

35. D'Halluin F, Tas P, Rouquette S, et al. Intra-operative touch preparation cytology following lumpectomy for breast cancer: a series of 400 procedures. Breast. 2009;18(4):248-53.

36. Erickson-Bhatt SJ, Nolan RM, Shemonski ND, et al. Real-time Imaging of the Resection Bed Using a Handheld Probe to Reduce Incidence of Microscopic Positive Margins in Cancer Surgery. Cancer Res. 2015;75(18):3706-12.

37. Santamaria G, Velasco M, Farrus B, et al. Preoperative MRI of pure intraductal breast carcinoma--a valuable adjunct to mammography in assessing cancer extent. Breast. 2008;17(2):186-94.

38. Amano G, Ohuchi N, Ishibashi T, et al. Correlation of three-dimensional magnetic resonance imaging with precise histopathological map concerning carcinoma extension in the breast. Breast Cancer Res Treat. 2000;60(1):43-55.

39. Kim SA, Cho N, Ryu EB, et al. Background parenchymal signal enhancement ratio at preoperative MR imaging: association with subsequent local recurrence in patients with ductal carcinoma in situ after breast conservation surgery. Radiology. 2014;270(3):699-707.

40. Somerville JE, Clarke LA, Biggart JD**.** c-erbB-2 overexpression and histological type of in situ and invasive breast carcinoma. J Clin Pathol. 1992;45(1):16-20.

41. Park K, Han S, Kim HJ, et al. HER2 status in pure ductal carcinoma in situ and in the intraductal and invasive components of invasive ductal carcinoma determined by fluorescence in situ hybridization and immunohistochemistry. Histopathology. 2006;48(6):702-7.

42. Allred DC, Clark GM, Molina R, et al. Overexpression of HER-2/neu and its relationship with other prognostic factors change during the progression of in situ to invasive breast cancer. Hum Pathol. 1992;23(9):974-9.

43. Harada S, Mick R, Roses RE, et al. The significance of HER-2/neu receptor positivity and immunophenotype in ductal carcinoma in situ with early invasive disease. J Surg Oncol. 2011;104(5):458-65.

44. Wang SY, Shamliyan T, Virnig BA, Kane R**.** Tumor characteristics as predictors of local recurrence after treatment of ductal carcinoma in situ: a meta-analysis. Breast Cancer Res Treat. 2011;127(1):1-14.

45. Park CC, Rembert J, Chew K, et al. High mammographic breast density is independent predictor of local but not distant recurrence after lumpectomy and radiotherapy for invasive breast cancer. Int J Radiat Oncol Biol Phys. 2009;73(1):75-9.

46. Chen X, Yuan Y, Gu Z, Shen K**.** Accuracy of estrogen receptor, progesterone receptor, and HER2 status between core needle and open excision biopsy in breast cancer: a meta-analysis. Breast Cancer Res Treat. 2012;134(3):957-67.

47. Dzierzanowski M, Melville KA, Barnes PJ, et al. Ductal carcinoma in situ in core biopsies containing invasive breast cancer: correlation with extensive intraductal component and lumpectomy margins. J Surg Oncol. 2005;90(2):71-6.

48. Partridge SC, McDonald ES**.** Diffusion weighted magnetic resonance imaging of the breast: protocol optimization, interpretation, and clinical applications. Magn Reson Imaging Clin N Am. 2013;21(3):601-24.

49. Bickel H, Pinker-Domenig K, Bogner W, et al. Quantitative apparent diffusion coefficient as a noninvasive imaging biomarker for the differentiation of invasive breast cancer and ductal carcinoma in situ. Invest Radiol. 2015;50(2):95-100.

50. Barentsz MW, Taviani V, Chang JM, et al. Assessment of tumor morphology on diffusion-weighted (DWI) breast MRI: Diagnostic value of reduced field of view DWI. J Magn Reson Imaging. 2015.

Figures

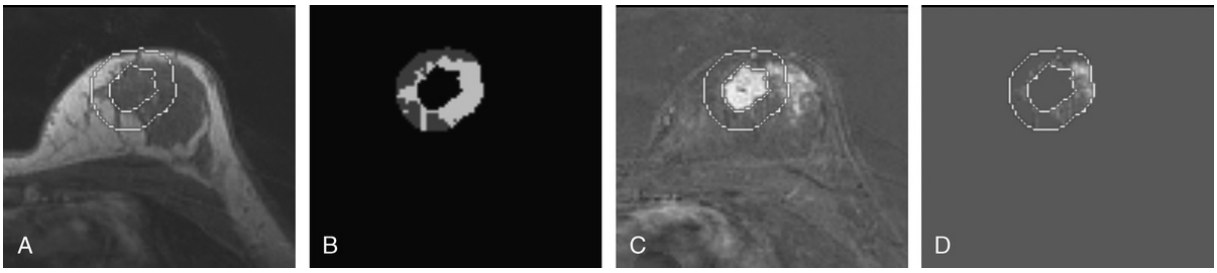

Figure 1 Axial MR-slices through invasive ductal carcinoma with surrounding E-DCIS in left breast. **A** Pre-contrast T1-weighted non-fat suppressed image, inner white line indicates tumor border and outer white line indicates automatically extended margin of 10 mm. **B** Segmentation of 10 mm margin into fibroglandular tissue (white) and adipose tissue (grey). The proportion of fibroglandular tissue is high, indicating high tissue density. **C** Subtraction of the first post-contrast scan minus the pre-contrast scan. **D** The relative signal increase between the pre-contrast and first post-contrast scan in the 10 mm extended margin around the MRI-visible lesion.

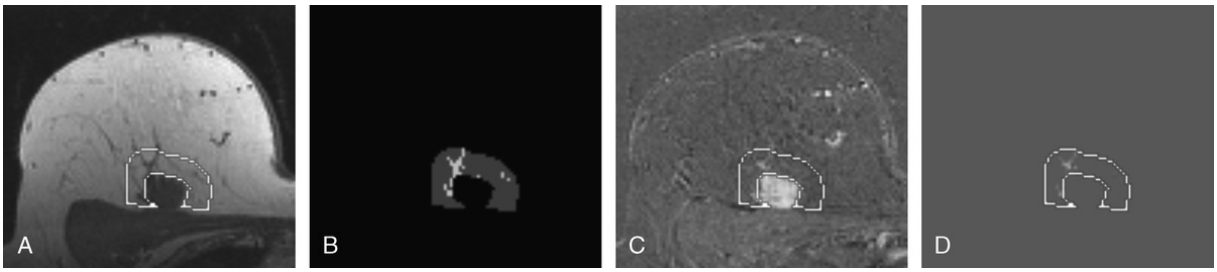

Figure 2 Axial MR-slices through invasive ductal carcinoma without surrounding E-DCIS in right breast. **A** Pre-contrast T1-weighted non-fat suppressed image, inner white line indicates tumor border and outer white line indicates automatically extended margin of 10 mm. Note that the pectoral muscle is automatically segmented as well, and omitted from the extended margin. **B** Segmentation of 10 mm margin into fibroglandular tissue (white) and adipose tissue (grey). The proportion of adipose tissue is high, indicating low tissue density. **C** Subtraction of the first post-contrast scan minus the pre-contrast scan. **D** The relative signal increase between the pre-contrast and first post-contrast scan in the 10 mm extended margin around the MRI-visible lesion.

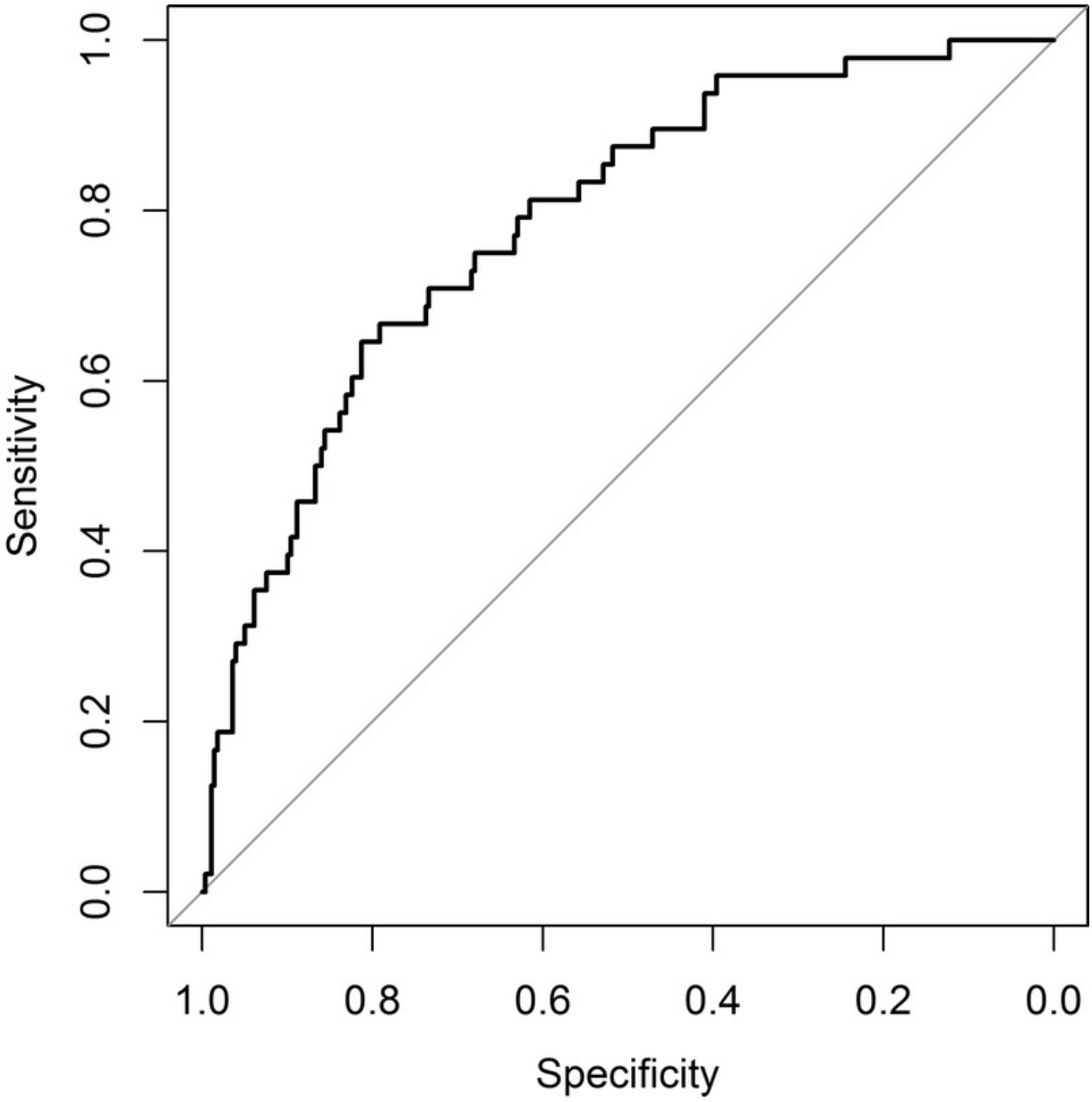

Figure 3 Apparent receiver operating characteristic curve of the prediction model based on the five components with eigenvalue larger than 1.0 yielded by principal component analysis. The area under the curve is 0.79 (95%-CI 0.72 - 0.85).

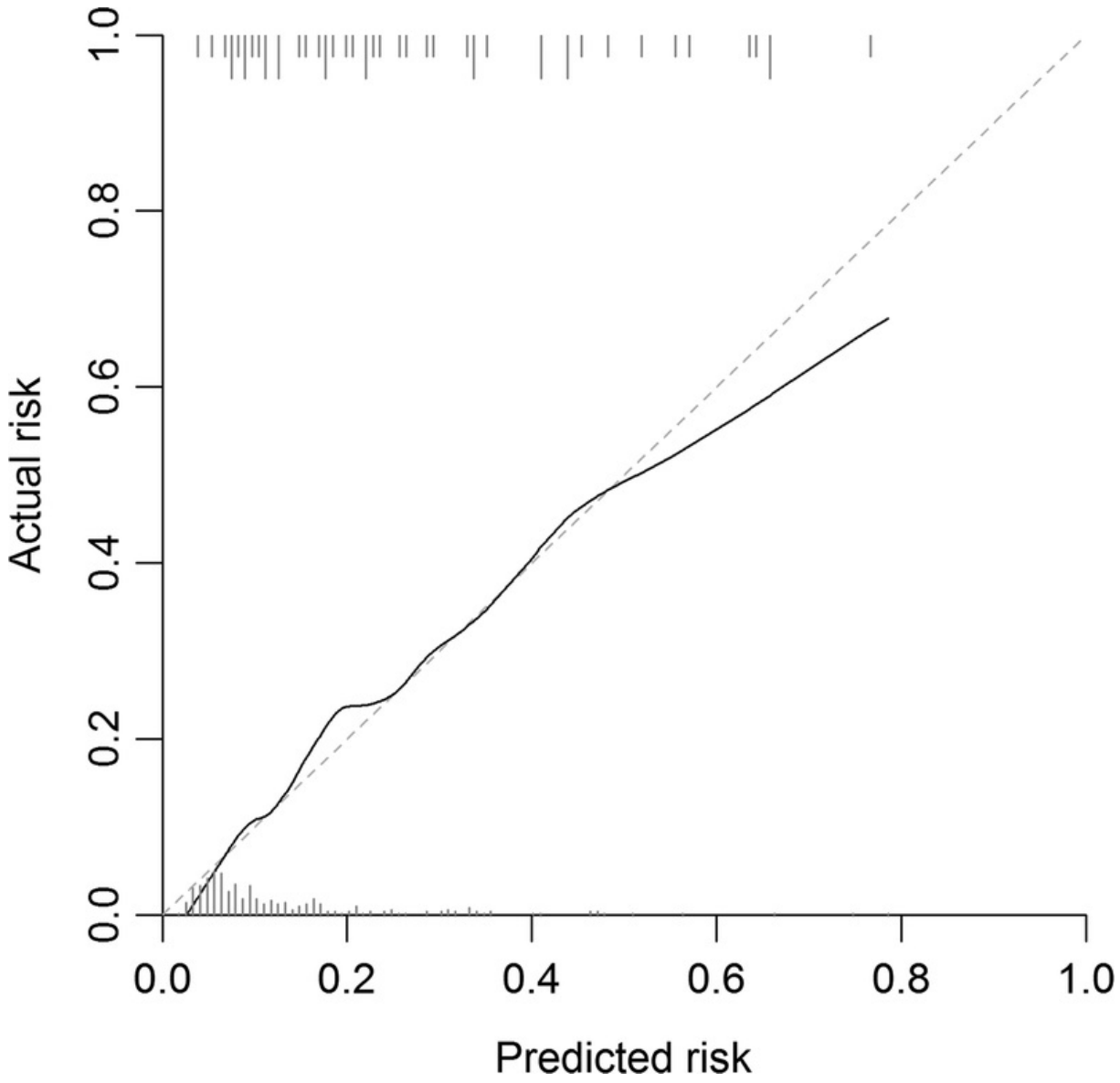

Figure 4 Apparent calibration curve showing the predicted risk of extensive ductal carcinoma in situ plotted against the actual risk. The grey bars represent distribution of predicted risk of women with (actual risk = 1.0) and without (actual risk = 0.0) extensive ductal carcinoma in situ.